LIMNOLOGY
and
OCEANOGRAPHY: METHODS

ASLO

Limnol. Oceanogr.: Methods 22, 2024, 25–33
© 2023 Association for the Sciences of Limnology and Oceanography.
doi: 10.1002/lom3.10589

Lab-based multispectral photography for approximating chlorophyll content in *Zostera marina*

Katherine Ann Haviland,[1,2]* **Melanie Hayn**,[1,2,3] **Robert Warren Howarth**[1,2,3]

[1]Cornell University Field of Natural Resources, Ithaca, New York, USA
[2]Cornell University Department of Ecology & Evolutionary Biology, Ithaca, New York, USA
[3]Marine Biological Laboratory, Woods Hole, Massachusetts, USA

Abstract

Reduced light is one of the primary threats to seagrass meadows in the coming decades, with reduced light reaching the benthos due to eutrophication. We assessed a multispectral photography technique using near-infrared photography to estimate chlorophyll content in the seagrass *Zostera marina*. Using near-infrared and red wavelength cameras in the lab environment, we measured normalized difference vegetation index (NDVI) in photographs of sampled seagrass leaves. In samples taken from three different environments, we found a positive correlation between lab-based NDVI and chlorophyll content, with variation attributable to leaf age. In samples grown under different light conditions, we found high levels of NDVI associated with lower light possibly due to seagrass photoacclimation. This method may be used in addition to existing seagrass monitoring methods to collect data on seagrass photic status and estimate chlorophyll content, and detect possible light limitation due to turbidity or high epibiota cover. The relatively low cost and time required for this method may make it useful where researchers are already collecting and imaging seagrass as part of routine monitoring.

Leaf chlorophyll content is a metric commonly used in seagrass monitoring and can provide information on possible plant photoacclimation (Longstaff and Dennison 1999; Fokeera-Wahedally and Bhikajee 2005), leaf senescence and maturity (Lichtenthaler and Babani 2004), and broadly, plant health (Biber et al. 2005; Rotini et al. 2013; Yang et al. 2018). In the last century, seagrass meadows have experienced multiple stressors, including eutrophication (Howarth et al. 2000; Haviland et al. 2022), as well as disease, coastal engineering, physical damage from boat propellers, and increased storm severity as a result of global climate change (Orth et al. 2006). Waycott et al. (2009) estimate that over 51,000 km^2 of seagrass meadow area have been lost between 1879 and 2006. In eutrophic conditions, seagrass must tolerate high levels of light limitation resulting from increased turbidity and shading by macroalgae and epibiota cover (Valiela et al. 1997). Dennison and Alberte (1986) found that seagrass produce greater leaf chlorophyll in response to decreased light.

Many terrestrial researchers use airborne remote sensing techniques to estimate leaf chlorophyll content through multispectral and hyperspectral photography. Submerged subtidal vegetation along turbid coastlines is difficult to assess in this way at a fine scale (Wicaksono and Hafizt 2013). Major challenges to traditional remote sensing techniques include interference by suspended and benthic algae, presence of dead vegetation, turbidity, and epibiota cover, and as a result require significant ground-truthing to develop accurate estimates of seagrass presence (Hedley et al. 2016). Along eutrophic temperate coastlines where turbidity is continuously high, remote sensing of seagrass can be even more technologically challenging (Kim et al. 2015). However, spectral reflectance can still be a useful metric of seagrass health. The near-infrared (NIR) waveband, from 750 to 950 nm, has been successfully used to quantify seagrass tissue composition (Bain et al. 2013), nutrient composition (Lawler et al. 2006), aboveground biomass (Costa et al. 2021), and leaf tissue photosynthetic properties (Durako 2007) in lab and field environments. Like their terrestrial counterparts, seagrass exhibit a characteristic red edge reflectance spectrum, with a marked increase in reflectance at 750+ nm (Horler et al., 2007; Thorhaug et al. 2007). Red light (600–700 nm) is highly absorbed by chlorophyll *a* and *b* (Chl *a* and Chl *b*) for use in photosynthesis, creating a characteristic dip in reflectance of red light in healthy vegetation (Huete 2004). This pattern of reflectance can be exploited to calculate vegetation indices such as normalized

*Correspondence: kah334@cornell.edu

Author Contribution Statement: The authors contributed to the manuscript by assisting with the development of the method (KH, MH, RH), image analysis (KH), statistical analyses on the dataset (KH), and the creation and polishing of the manuscript (KH, MH, RH).

Additional Supporting Information may be found in the online version of this article.

difference vegetation index (NDVI). NDVI is a classic index consisting of NIR reflectivity (750+ nm) normalized to red waveband reflectivity (600–700 nm) developed by Tucker et al. (1985). Increased chlorophyll content corresponds to reduced reflectance of red light (Fyfe 2003) and a greater NDVI value.

In this paper, we assess the use of this spectral vegetation index, NDVI, as an inexpensive, non-destructive estimate of chlorophyll content on harvested *Zostera marina*, measured in a controlled laboratory environment. We tested this method on seagrass (*Z. marina*) harvested along a gradient of environmental stressors, including epibiota cover and porewater sulfide levels, and a separate population of plants harvested from one location and grown in a mesocosm environment under varying light conditions.

Materials and procedures

Study site and sample harvest

West Falmouth Harbor (WFH) is a shallow (mean depth at mean high tide of 1.9 m) lagoon adjoining Buzzards Bay in Falmouth, MA, on Cape Cod (USA). For a detailed description of WFH, see Hayn et al. (2014), and Howarth et al. (2014). WFH can be divided into sub-basins existing along a gradient of nutrient enrichment, with the Middle Harbor basin being more nitrogen-impacted than the seaward Outer Harbor basin. Both the Middle Harbor and Outer Harbor basins contain dense, subtidal, monospecific meadows of *Zostera marina*. However, seagrass in the Middle Harbor basin face greater environmental stressors than those in the Outer Harbor, notably high epibiota biomass and porewater sulfide concentrations approaching thresholds for seagrass toxicity (Haviland et al. 2022).

In July of 2018 and again in 2019, we harvested seagrass from nine sites across the Middle and Outer Harbor basins of WFH, five in the Middle Harbor region, and four in the Outer Harbor region. SCUBA divers harvested 10 entire plants from each long-term study site. At all sample sites, divers measured seagrass density by counting the number of shoots in a quarter m^2 quadrat three times. Additional seagrass shoots were collected from less nutrient-impacted sites in Buzzards Bay just outside West Falmouth Harbor (referred to as "external sites"). In August 2018, to assess intra-site spatial heterogeneity and the effect of small differences in depth on lab-based NDVI, we collected seagrass from two locations within 5 m of each other, the major difference being depth. To assess the sensitivity of the measurement to small changes in depth within the bounds of each site, we identified locations differing by a depth of 0.1–0.25 m, and collected 10 plants each from the two depth classes. All plants were harvested and processed using identical methods, described in "sample processing" below.

In June–August 2021, 4 groups of 32 seagrass each (total $n = 128$) were harvested from the same location within WFH and planted in flow-through seawater tanks. The tanks were 2.6 m^3 (2.7 m × 1.2 m × 0.8 m, $l \times w \times d$), and received a constant flow of unfiltered, low-nutrient seawater from Vineyard Sound. Shades were hung over each tank to achieve between 50% and 80% reduction in ambient light. Plants in the highest light exposure received on average 244 μmol m^{-2} s^{-1} photosynthetic photon flux density (PPFD) in integrated daylight photosynthetically active radiation (PAR), while plants in the two middle tanks received 178 and 189 μmol m^{-2} s^{-1}, and plants in the darkest tank received 137 μmol m^{-2} s^{-1}. Light conditions at the site from which seagrass were harvested ranged from 300 to 500 μmol m^{-2} s^{-1} (del Barrio et al. 2014). PAR was measured once weekly using a submersible LICOR with a spherical sensor, measured underwater at the canopy level, while light was also monitored continuously using Onset HOBO Pendant loggers in each tank suspended at the seagrass canopy level. All plants were collected after 8 weeks and processed using the methods described below on the same day of collection, except for plants from the 137 μmol m^{-2} s^{-1} group, which were removed from analysis due to browning of leaf tips resulting from a delay between sampling and imaging.

Sample processing

Seagrass samples with rhizomes intact were kept in bags of site water on ice during travel to the Marine Biological Lab in Woods Hole, MA (~ 13 km from sampling site), for imaging and chlorophyll preprocessing. Within 24 h of sampling (most within 6 h), all plants were processed and photographed using a dark box and fitted camera rig, described below. Immediately after imaging, plants were frozen at −80°C pending chlorophyll analysis; for all plants, less than 24 h passed between sampling and freezing, and plants stayed in cold site water for this entire period. Leaves from individual plants were assessed according to leaf age (the youngest leaf is assigned leaf 1, second youngest leaf 2, and so on). Seagrass were placed in distilled water, then carefully scraped to remove epibiota; we placed epibiota in pre-weighed tins and moved them to a drying oven at 60°C for 3 d. We then placed seagrass leaves in age-order on labeled transparency sheets, and patted leaves dry to prevent pooling of water and glare on the image. The transparency containing the seagrass was then moved into a dark box (Fig. 1). The box was made of a metal frame and white polystyrene sides and was 66 cm high by 20 in. wide by 28 cm long. At approximately 30 cm height, we suspended light diffusion paper to ensure equal distribution of light across the samples; an 8 cm diameter hole in the diffusion paper ensured the camera could collect a clear image without interference. The ceiling of the box contained two sets of NIR-emitting LED lamp strips (emitting at 850 nm), and two sets of red LED lamp strips (emitting at 660 nm). We then photographed seagrass within the box using a dual-camera set-up: an Agrocam NDVI Pro NIR-G-B camera capturing ~ 750 nm wavelength for NIR, and a GitUp Git 2 Pro action camera equipped with an Agrocam RGB lens capturing ~ 650 nm red. Images were captured successively by removing one camera, and then adding the next, to the camera rig. At the beginning

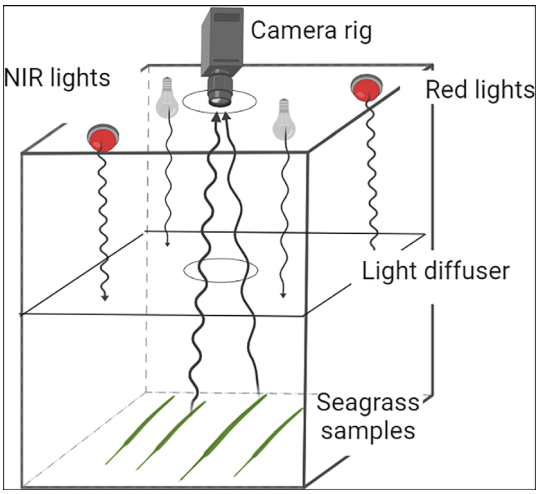

Fig. 1. A schematic representation of the light-box setup used to photograph seagrass under standardized light conditions, created using Blender. We used two NIR light strips, and two red wavelength LED strips (all ~ 10 cm long each) fixed to the top of the box.

and end of each day, we photographed a color-standardization card to ensure image capture and lighting did not change throughout the study.

Following imaging, we placed seagrass in foil packets and froze them at −80°C pending chlorophyll content analysis. Within a year (analysis was delayed on summer 2019 samples due to the COVID-19 pandemic), seagrass were analyzed for chlorophyll content using the method described by Dennison (1990). Briefly, we soaked 5 cm^2 of seagrass leaf for 10 min in 3 mL 100% acetone, ground the samples in an ice bath in a dark hood using a mortar and pestle, added 10 mL of 80% acetone/20% nano-pure distilled water solution per cm^2 leaf area, and then analyzed on a spectrophotometer at 663, 645, and 720 nm. Chl *a* and Chl *b* were estimated using the equations developed by Arnon (1949). In order to make the most appropriate comparisons of chlorophyll content and leaf-average NDVI, we measured chlorophyll on several different locations along the leaf for chlorophyll content (tip, top-middle, bottom-middle, and base of the plant) on a subset of plants to determine which location along the leaf on which to focus analysis, finding that on average, chlorophyll content was highest in the middle segments of a leaf, lowest at the base, and close to the leaf average at the tip. Because of this, we chose to use only plant tips for the remaining chlorophyll analysis, and assessed chlorophyll content on the top 5 cm^2 of all leaves.

Image analysis

We used the ArcGIS software suite to analyze our seagrass images. We first standardized light levels from each day by normalizing all pixel values to the color standardization card. For additional accuracy, leaves may be laid directly on top of reflectance cards, and light output may be standardized for each image. Images from the two cameras were blended together using ArcGIS Pro's Georeference tool, selecting eight matching pixels along the edge and tip of blades throughout both images. Once the images were aligned, they were combined into a two-band raster, with the first layer containing the NIR image, and the second layer containing the red image. We detected and measured leaf area using unsupervised pixel classification, followed by manual selection of leaf area, where unsupervised classification failed. Supervised classification of leaf area may be an option for future development of this method. We then clipped images so only the pixels containing seagrass area were within the image. We then created an NDVI raster through the equation: $(NIR_{750} - Red_{650})/(NIR_{750} + Red_{650})$, and recorded, for each leaf on each plant, an average pixel NDVI value, as well as a minimum and maximum pixel value, and a standard deviation for each leaf using the ArcGIS Zonal Statistics tool. The full resulting dataset is available in Supporting Information Table S1.

Notably, this method can be carried out in any image analysis software capable of raster analysis (ImageJ, QGIS, ENVI, Adobe Photoshop, Domo, etc.), if the cost of an ArcGIS license or software training presents a barrier.

Statistical analysis

We assessed the relationship between Chl *a* and Chl *b* content and NDVI in a simple linear regression using seagrass samples collected from West Falmouth Harbor and sites just outside of West Falmouth Harbor in 2018 and 2019 after testing for model assumptions including normality and heteroscedasticity. We randomly separated the dataset into training and test data with a 70–30 split. We created and tested the model using the olsrr (Hebbali 2020) and caTools (Tuszynski 2021) packages in the R computing environment, using tidyverse techniques (Wickham et al. 2019). We assessed NDVI under the various shade treatments in the mesocosm experiment using Tukey's multiple comparison of means test.

Assessment

NDVI and seagrass morphometry

Leaf average NDVI spanned ~ 0 to +0.20 in all plants sampled, with an average of 0.10, while chlorophyll content spanned 0.5–30 μg chlorophyll per cm^2 leaf area, and did not significantly differ between 2018 and 2019.

Leaf average NDVI positively correlated with Chl *a* + Chl *b* content as expected ($p < 0.001$) (Fig. 2). The second- and third-youngest leaves (leaves 2 and 3) regularly showed the highest values for NDVI as well as chlorophyll content. The relationship between NDVI and chlorophyll content followed the equation:

$$Chl_{a+b} = 1.9 + 93.5\,(NDVI)$$

where Chl_{a+b} refers to Chl *a* and Chl *b* content in μg chlorophyll per cm^2 seagrass leaf area (double-sided), and NDVI

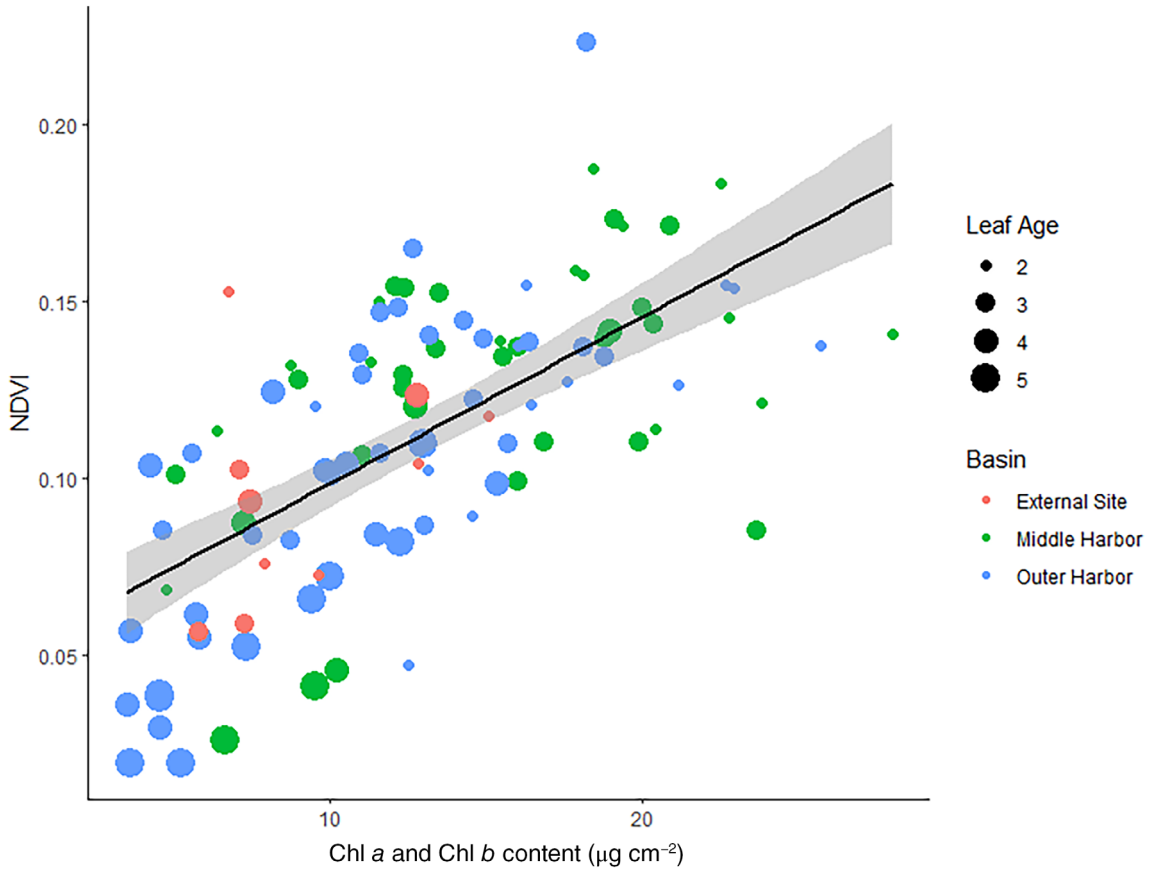

Fig. 2. Chlorophyll content and whole-plant average NDVI in seagrass harvested in July of 2018 and 2019 ($p < 2.2 \times 10^{-16}$). Figure includes all seagrass sampled from WFH and external sties. Gray shading represents the 95% confidence interval. NDVI was corrected in 2019 due to the NIR light-bulbs dimming with age, quantified using image standardization cards. For full regression analysis information, see Supporting Information Fig. S1 and Table S1.

refers to plant average NDVI value. Single-sided leaf area may also be used, resulting in a doubling of the intercept and slope. The root mean squared error of the model is 4.13 μg per cm^2 (Fig. 3). Model residuals were normally distributed and are reported in Supporting Information Fig. S1. The model performed best for estimating the chlorophyll content of leaf ages 2–5, and at estimating chlorophyll contents between 5 and 20 μg cm^{-2}.

NDVI varied along the leaf surface, with peak values generally exhibited in the upper half of the seagrass leaf. Supporting Information Fig. S2 represents an example output of variation along the length of seagrass leaves and leaf ages, with highest values seen in the middle-aged leaves (Fig. 4), near the tips of the leaves. The pattern we see reflects typical variation found on the surface of seagrass leaves: the base of the leaf represents the youngest part of the leaf, where chloroplasts are still developing and the greatest self-shading occurs, and the leaf tip is the oldest part of the leaf, often heavily colonized by epiphytes and the first to experience senescence and chlorophyll degradation as the plant ages (Enríquez et al. 2002; Ralph et al. 2005).

As this method allows us to sample variation in light reflectance along the entire leaf surface, we noted a pattern within most plants where peak NDVI levels in the highest reflectance leaves (leaves 2 and 3) were found toward the middle of the leaf, generally 30–40% downwards from the tip of the leaf. In older leaves (leaves 4 and 5), NDVI also followed this pattern, but often had a second peak reflectance value closer to the leaf tip. See the Supporting Information for an example of a characteristic plant showing these patterns (Supporting Information Fig. S2).

NDVI and light environment

In the mesocosm experiment, we found the highest levels of NDVI in seagrass grown under low-light conditions, possibly due to photoacclimation, where seagrass chlorophyll content increases as solar irradiance decreases (Dennison and Alberte 1982; Dennison and Alberte 1986; Abal et al. 1994; Longstaff and Dennison 1999). Seagrass NDVI decreased with light (Fig. 5, $p = 0.0006$), and was highest at the light class receiving the least light, at 137 μmol m^{-2} s^{-1} PPFD over the daylight period. This number (which converts to

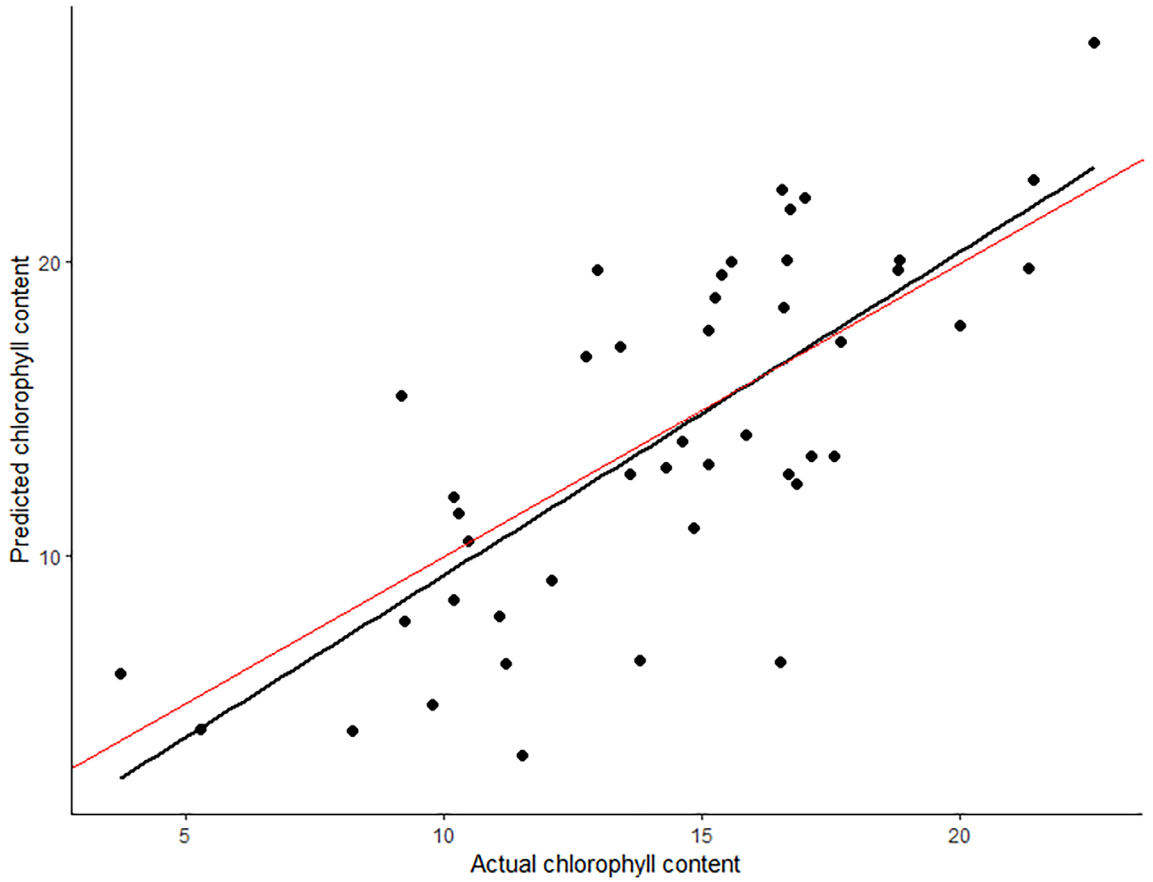

Fig. 3. Chl a + Chl b content (μg cm^{-2} leaf area) predicted using NDVI method (y-axis) vs. actual Chl a + Chl b content (RMSE = 4.13, R^2 = 0.57) on test data set. The black line represents the modeled relationship (Fig. 2), while the red line represents the line of perfect agreement ($y = x$).

~6.2 mol m^{-2} d^{-1}) approaches the threshold value for light below which Collier et al. (2009) began to see declines in seagrass cover. Epibiota biomass did not affect NDVI in any light class ($p > 0.1$ for all).

Variation in water depth within a sampling site was not a significant predictor of NDVI at any site ($p > 0.1$), possibly due to the relatively small differences in depth within each site not resulting in substantially different light intensities. Typical attenuation coefficients at this site are 0.45 m^{-1} (del Barrio et al. 2014). Our differences in depth (0.1–0.25 m) thus correspond to attenuation of ~ 17.6–44 μmol m^{-2} s^{-1}. This may in fact be negligible when compared to typical light levels in the canopy (300–500 μmol m^{-2} s^{-1}).

Discussion

Our method approximates seagrass chlorophyll content in a way that once set up, takes less time than traditional spectrophotometric methods, and does not consume the sample, allowing other analyses such as isotopic or genetic measurements to be carried out on the same seagrass leaves for a more statistically robust sample. It can be carried out quickly and inexpensively (< 700 USD as of 2019) as an addition to ongoing seagrass monitoring operations, where seagrass samples are already harvested for laboratory analysis. Because of the low time commitment and cost associated with this method compared to traditional methods, multispectral photography is a useful addition to the monitoring campaigns undertaken by scientists who are already collecting and imaging seagrass for different metrics like tracking wasting disease (Graham et al. 2021), grazing (Kirsch et al. 2002), and leaf area (de los Santos et al. 2016). As each pixel represents a leaf area region < 0.0001 cm^2, this method gives us a detailed understanding of chlorophyll content along the entire blade. The addition of multispectral information to regular monitoring tasks, and comparison of the results within a site, may help provide some evidence of photoacclimation to low light, which can be an early indicator of potential bed loss as a result of eutrophication (Biber et al. 2009). This method, when combined with additional monitoring technique that assess photosynthetic activity, can help coastal managers make informed decision regarding operations that further reduce light penetration such as shell fishing, dredging, and additional nutrient pollution.

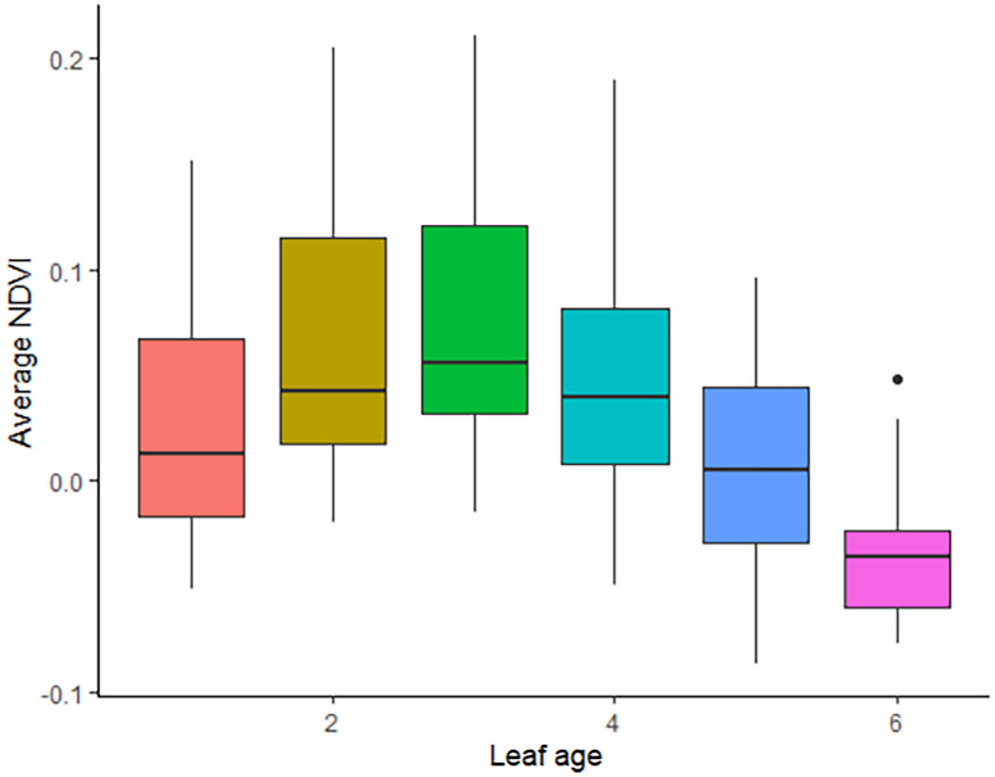

Fig. 4. Relationship between average leaf NDVI and leaf age, where a leaf of 1 indicates the youngest leaf on a plant, and 6 is the oldest. While some plants had a seventh or eighth leaf, those values were excluded from this analysis due to their small sample size.

While there is imprecision in the relationship between chlorophyll content and NDVI (Fig. 2), the multispectral photography method may be beneficial over traditional chlorophyll content analysis for researchers in some situations. Multispectral photography gives a detailed view of chlorophyll content along the entire seagrass plant, showing regions of high NIR reflectivity and demonstrating small-scale spatial heterogeneity in light usage along the seagrass leaf. Prior work has shown chlorophyll content to be greatest in the middle-section of seagrass leaves compared to the apical section (Dalla Via et al. 1998) and the bottom, where tissues are immature (Ralph et al. 2005), which we also see with this method. As chlorophyll content analyses are typically carried out only on small segments of a plant, this multispectral method may present a more holistic understanding of light usage dynamics within the whole plant. In addition, the images captured can be stored indefinitely and processed at any time. Because multiple analyses can be carried out using one plant sample, the number of seagrass plants harvested can be minimized, protecting the integrity of seagrass meadows, many of which are already at risk of ecosystem degradation (Turschwell et al. 2021). While small handheld chlorophyll samplers are also an inexpensive option for researchers looking to map seagrass chlorophyll content on the leaf (Yuan et al. 2016), and have similar precision to our method, the multispectral photography method we present here may be a useful option for researchers looking to map multiple plants more efficiently. We recommend, however, that researchers using this method first develop a standard curve between NDVI and chlorophyll content by analyzing 20–30 leaves for both chlorophyll content and NDVI.

Future climate scenarios predict enhanced eutrophication in many coastal regions due to increased precipitation and nitrogen fluxes (Sinha et al. 2017), reducing light reaching seagrass meadows. As a result of decreased light and other anthropogenic stressors, seagrass in some regions, including New England where this study was carried out, face significant risk of a rapid decline in the coming decades (Turschwell et al. 2021). Beyond changes in the light environment, climate change may also impact seagrass leaf pigment through ocean acidification (Zimmerman et al. 2017; Celebi-Ergin et al. 2021). Monitoring seagrass health will become increasingly important to protecting seagrass meadow ecosystems as stressors on estuarine and coastal environments increase. The method presented here can be used as a tool to assess how seagrass interact with their light environment and may help mangers better identify seagrass at risk of mortality due to light limitation. Further testing on various seagrass species and on plants sampled from new locations, as well as modifications to the analysis, will continue to strengthen the

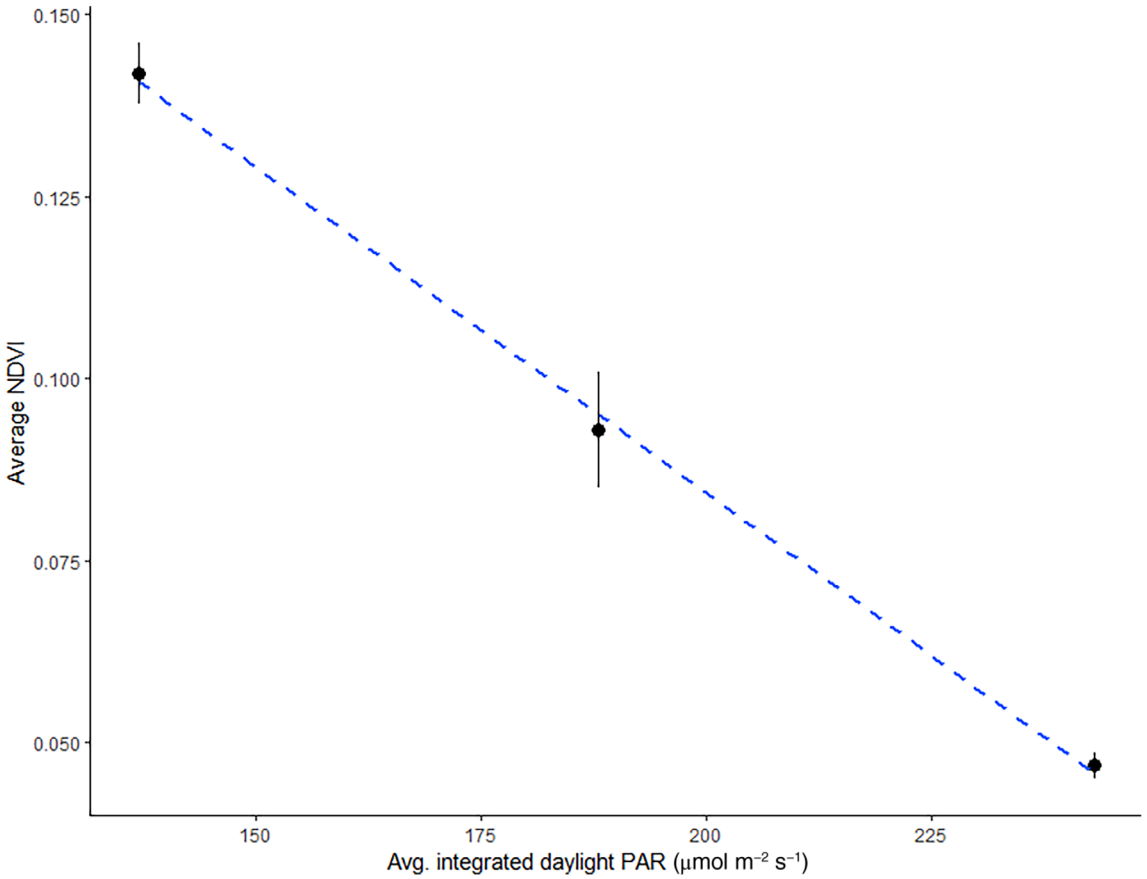

Fig. 5. Average plant NDVI under different shading treatments in a mesocosm environment. NDVI (average of third-youngest blades from ~ 40 plants grown under given light condition) decreases with increased light ($p = 0.0006$, df = 30). The black point represents the mean value for the group, while the black vertical line represents one standard error above and below the mean. Note that one light treatment (~ 175 μM) was removed from the analysis due to significant time between sampling and imaging (> 24 h) resulting in browning of leaves.

method. Additional testing on the effect of seagrass depth on NDVI, as well as potential modifications for use in the field, are avenues for future development of this method.

References

Abal, E. G., N. Loneragan, P. Bowen, C. J. Perry, J. W. Udy, and W. C. Dennison. 1994. Physiological and morphological responses of the seagrass *Zostera capricorni Aschers*, to light intensity. J. Exp. Mar. Biol. Ecol. **178**: 113–129. doi:10.1016/0022-0981(94)90228-3

Arnon, D. I. (1949). Copper enzymes in isolated chloroplasts. Polyphenoloxidase in Beta vulgaris. Plant physiology, **24**. doi:10.1073/pnas.2110802118

Bain, K. F., A. Vergés, and A. G. Poore. 2013. Using near infra red reflectance spectroscopy (NIRS) to quantify tissue composition in the seagrass *Posidonia australis*. Aquat. Bot. **111**: 66–70. doi:10.1016/j.aquabot.2013.05.012

Biber, P. D., H. W. Paerl, C. L. Gallegos, and W. J. Kenworthy. 2005. Evaluating indicators of seagrass stress to light. Estuar. Indic, p. 215–232.

Biber, P. D., W. J. Kenworthy, and H. W. Paerl. 2009. Experimental analysis of the response and recovery of *Zostera marina* (L.) and *Halodule wrightii* (Ascher.) to repeated light-limitation stress. J. Exp. Mar. Biol. Ecol. **369**: 110–117. doi:10.1016/j.jembe.2008.10.031

Celebi-Ergin, B., R. C. Zimmerman, and V. J. Hill. 2021. Impact of ocean carbonation on long-term regulation of light harvesting in eelgrass *Zostera marina*. Mar. Ecol. Prog. Ser. **671**: 111–128. doi:10.3354/meps13777

Collier, C. J., P. S. Lavery, P. J. Ralph, and R. J. Masini. 2009. Shade-induced response and recovery of the seagrass *Posidonia sinuosa*. J. Exp. Mar. Biol. Ecol. **370**: 89–103. doi:10.1016/j.jembe.2008.12.003

Costa, V., J. Serôdio, A. I. Lillebø, and A. I. Sousa. 2021. Use of hyperspectral reflectance to non-destructively estimate seagrass *Zostera noltei* biomass. Ecol. Indic. **121**: 107018. doi:10.1016/j.ecolind.2020.107018

Dalla Via, J., C. Sturmbauer, G. Schönweger, E. Sötz, S. Mathekowitsch, M. Stifter, and R. Rieger. (1998). Light gradients and meadow structure in Posidonia oceanica: ecomorphological and functional correlates. Marine

Ecology Progress Series, **163**: 267–278. doi:10.3354/meps163267

De los Santos, C. B., and others. 2016. A comprehensive analysis of mechanical and morphological traits in temperate and tropical seagrass species. Mar. Ecol. Prog. Ser. **551**: 81–94. doi:10.3354/meps11717

del Barrio, P., N. K. Ganju, A. L. Aretxabaleta, M. Hayn, A. García, and R. W. Howarth. 2014. Modeling future scenarios of light attenuation and potential seagrass success in a eutrophic estuary. Estuar. Coast. Shelf Sci. **149**: 13–23. doi:10.1016/j.ecss.2014.07.005

Dennison, W. C. 1990. Chlorophyll content. Seagrass research methods. UNESCO, p. 83–85.

Dennison, W. C., and R. S. Alberte. 1982. Photosynthetic responses of *Zostera marina* L.(eelgrass) to in situ manipulations of light intensity. Oecologia **55**: 137–144. doi:10.1007/BF00384478

Dennison, W. C., and R. S. Alberte. 1986. Photoadaptation and growth of *Zostera marina* L.(eelgrass) transplants along a depth gradient. J. Exp. Mar. Biol. Ecol. **98**: 265–282. doi:10.1016/0022-0981(86)90217-0

Durako, M. J. 2007. Leaf optical properties and photosynthetic leaf absorptances in several Australian seagrasses. Aquat. Bot. **87**: 83–89. doi:10.1016/j.aquabot.2007.03.005

Enríquez, S., M. Merino, and R. Iglesias-Prieto. 2002. Variations in the photosynthetic performance along the leaves of the tropical seagrass *Thalassia testudinum*. Mar. Biol. **140**: 891–900. doi:10.1007/s00227-001-0760-y

Fokeera-Wahedally, S. B. M., and M. Bhikajee. 2005. The effects of in situ shading on the growth of a seagrass, *Syringodium isoetifolium*. Estuar. Coast. Shelf Sci. **64**: 149–155. doi:10.1016/j.ecss.2005.01.006

Fyfe, S. K. 2003. Spatial and temporal variation in spectral reflectance: Are seagrass species spectrally distinct? Limnol. Oceanogr. **48**: 464–479. doi:10.4319/lo.2003.48.1_part_2.0464

Graham, O. J., and others. 2021. Effects of seagrass wasting disease on eelgrass growth and belowground sugar in natural meadows. Front. Mar. Sci. **8**: 768668. doi:10.3389/fmars.2021.768668

Haviland, K. A., R. W. Howarth, R. Marino, and M. Hayn. 2022. Variation in sediment and seagrass characteristics reflect multiple stressors along a nitrogen-enrichment gradient in a New England lagoon. Limnol. Oceanogr. **67**: 660–672. doi:10.1002/lno.12025

Hayn, M., and others. 2014. Exchange of nitrogen and phosphorus between a shallow lagoon and coastal waters. Estuar. Coast. **37**: 63–73. doi:10.1007/s12237-013-9699-8

Hebbali, A (2020). olsrr: Tools for building OLS regression models. R package version 0.5.3. Available from https://CRAN.R-project.org/package=olsrr

Hedley, J., B. Russell, K. Randolph, and H. Dierssen. 2016. A physics-based method for the remote sensing of seagrasses. Remote Sens. Environ. **174**: 134–147. doi:10.1016/j.rse.2015.12.001

Howarth, R. W., and others. 2000. Nutrient pollution of coastal rivers, bays, and seas. Issues Ecol. **7**: 1–16.

Howarth, R. W., and others. 2014. Metabolism of a nitrogen-enriched coastal marine lagoon during the summertime. Biogeochemistry **118**: 1–20. doi:10.1007/s10533-013-9901-x

Huete, A. R. 2004. Remote sensing for environmental monitoring, p. 183–206. *In* Environmental monitoring and characterization. Academic Press.

Kim, K., J. K. Choi, J. H. Ryu, H. J. Jeong, K. Lee, M. G. Park, and K. Y. Kim. 2015. Observation of typhoon-induced seagrass die-off using remote sensing. Estuar. Coast. Shelf Sci. **154**: 111–121. doi:10.1016/j.ecss.2014.12.036

Kirsch, K. D., J. F. Valentine, and K. L. Heck Jr. 2002. Parrotfish grazing on turtlegrass *Thalassia testudinum*: Evidence for the importance of seagrass consumption in food web dynamics of the Florida Keys National Marine Sanctuary. Mar. Ecol. Prog. Ser. **227**: 71–85. doi:10.3354/meps227071

Lawler, I. R., L. Aragones, N. Berding, H. Marsh, and W. Foley. 2006. Near-infrared reflectance spectroscopy is a rapid, cost-effective predictor of seagrass nutrients. J. Chem. Ecol. **32**: 1353–1365. doi:10.1007/s10886-006-9088-x

Lichtenthaler, H. K., and F. Babani. 2004. Light adaptation and senescence of the photosynthetic apparatus. Changes in pigment composition, chlorophyll fluorescence parameters and photosynthetic activity, p. 713–736. *In* Chlorophyll a fluorescence: A signature of photosynthesis. Springer Netherlands. doi:10.1007/978-1-4020-3218-9_28

Longstaff, B. J., and W. C. Dennison. 1999. Seagrass survival during pulsed turbidity events: The effects of light deprivation on the seagrasses *Halodule pinifolia* and H*alophila ovalis*. Aquat. Bot. **65**: 105–121. doi:10.1016/S0304-3770(99)00035-2

Orth, R. J., and others. 2006. A global crisis for seagrass ecosystems. Bioscience **56**: 987–996. doi:10.1641/0006-3568(2006)56[987:AGCFSE]2.0.CO;2

Ralph, P. J., C. M. O. Macinnis-Ng, and C. Frankart. 2005. Fluorescence imaging application: Effect of leaf age on seagrass photokinetics. Aquat. Bot. **81**: 69–84. doi:10.1016/j.aquabot.2004.11.003

Rotini, A., and others. 2013. Effectiveness and consistency of a suite of descriptors for assessing the ecological status of seagrass meadows (*Posidonia oceanica* L. Delile). Estuar. Coast. Shelf Sci. **130**: 252–259. doi:10.1016/j.ecss.2013.06.015

Sinha, E., A. M. Michalak, and V. Balaji. 2017. Eutrophication will increase during the 21st century as a result of precipitation changes. Science **357**: 405–408. doi:10.1126/science.aan2409

Thorhaug, A., A. D. Richardson, and G. P. Berlyn. 2007. Spectral reflectance of the seagrasses: *Thalassia testudinum*, *Halodule wrightii*, *Syringodium filiforme* and five marine algae. Int. J. Remote Sens. **28**: 1487–1501. doi:10.1080/01431160600954662

Tucker, C. J., C. L. Vanpraet, M. J. Sharman, and G. Van Ittersum. 1985. Satellite remote sensing of total herbaceous biomass production in the Senegalese Sahel: 1980–1984. Remote Sens. Environ. **17**: 233–249. doi:10.1016/0034-4257(85)90097-5

Turschwell, M. P., and others. 2021. Anthropogenic pressures and life history predict trajectories of seagrass meadow extent at a global scale. Proc. Natl. Acad. Sci. USA **11**: e2110802118. doi:10.1073/pnas.2110802118

Tuszynski, J. (2021). caTools: Tools: Moving window statistics, GIF, Base64, ROC AUC, etc. R package version 1.18.2. Available from https://CRAN.R-project.org/package=caTools

Valiela, I., J. McClelland, J. Hauxwell, P. J. Behr, D. Hersh, and K. Foreman. 1997. Macroalgal blooms in shallow estuaries: Controls and ecophysiological and ecosystem consequences. Limnol. Oceanogr. **42**: 1105–1118. doi:10.4319/lo.1997.42.5_part_2.1105

Waycott, M., and others. 2009. Accelerating loss of seagrasses across the globe threatens coastal ecosystems. Proc. Natl. Acad. Sci. USA **106**: 12377–12381. doi:10.1073/pnas.0905620106

Wicaksono, P., and M. Hafizt. 2013. Mapping seagrass from space: Addressing the complexity of seagrass LAI mapping. Eur. J. Remote Sens. **46**: 18–39. doi:10.5721/EuJRS20134602

Wickham, H., and others. 2019. Welcome to the Tidyverse. J. Open Source Softw. **4**: 1686. doi:10.21105/joss.01686

Yang, X., P. Zhang, W. Li, C. Hu, X. Zhang, and P. He. 2018. Evaluation of four seagrass species as early warning indicators for nitrogen overloading: Implications for eutrophic evaluation and ecosystem management. Sci. Total Environ. **635**: 1132–1143. doi:10.1016/j.scitotenv.2018.04.227

Yuan, Z., and others. 2016. Optimal leaf positions for SPAD meter measurement in rice. Front. Plant Sci. **7**: 719. doi:10.3389/fpls.2016.00719

Zimmerman, R. C., and others. 2017. Experimental impacts of climate warming and ocean carbonation on eelgrass *Zostera marina*. Mar. Ecol. Prog. Ser. **566**: 1–15. doi:10.3354/meps12051

Acknowledgments

We thank Roxanne Marino for her helpful feedback and advice on this paper. We also thank Eli Perrone and EP Oceanographic, LLC for assisting with the set-up of the NIR and red light box, including the 3D-printed camera holder, for assisting with camera specifications, and for providing image standardization cards. We thank our research assistants, Vera Gaddi (2018) and Audrey Vinton (2019 and 2021) for their help with seagrass collection and processing. We gratefully acknowledge as our funding sources: the National Science Foundation Biocomplexity, GRFP, and LTREB programs (grants 0420575, 1654845, and 2018241438), and the Woods Hole SeaGrant program. Robert Howarth's position at Cornell is supported through an endowment given by David R. Atkinson. In addition, funding was graciously provided by Cornell University's Andrew W. Mellon fund, Cornell University's Betty Miller Francis fund, and funding provided by the International Women's Fishing Association. We also thank three anonymous reviewers whose thorough and kind reviews greatly improved this paper.

Conflict of Interest

None declared.

Submitted 20 December 2022
Revised 13 October 2023
Accepted 17 October 2023

Associate editor: Tammi Richardson